



Effective exploration and visualization of geological parameter space

F. Boschetti

CSIRO Exploration and Mining, P.O. Box 1130, Bentley, Western Australia 6102, Australia (fabio.boschetti@csiro.au)

C. Wijns

CSIRO Exploration and Mining, P.O. Box 1130, Bentley, Western Australia 6102, Australia

Centre for Global Metallogeny, University of Western Australia, Crawley, Western Australia 6009, Australia

L. Moresi

CSIRO Exploration and Mining, P.O. Box 1130, Bentley, Western Australia 6102, Australia

Now at School of Mathematical Sciences, Monash University, Building 28, Victoria 3800, Australia

[1] Inverse modeling returns many solutions apart from the final product. Exploring and visualizing the solution space covered by an inversion leads to a greater understanding of the problem. Our method combines an inversion algorithm with an effective two-dimensional representation of the multidimensional model parameter space. The analysis of all solutions is done through a visualization technique known as self-organized mapping, resulting in a simple view of an otherwise complicated problem. A user may infer much about the controlling factors in the model through a few graphical displays of the data.

Components: 4792 words, 6 figures.

Keywords: numerical inversion; modeling; visualization.

Index Terms: 3260 Mathematical Geophysics: Inverse theory; 3210 Mathematical Geophysics: Modeling; 3230 Mathematical Geophysics: Numerical solutions.

Received 24 December 2002; **Revised** 22 May 2003; **Accepted** 25 June 2003; **Published** 15 October 2003.

Boschetti, F., C. Wijns, and L. Moresi, Effective exploration and visualization of geological parameter space, *Geochem. Geophys. Geosyst.*, 4(10), 1086, doi:10.1029/2002GC000503, 2003.

1. Introduction

[2] Geological modeling problems are often ill constrained, and it is therefore possible that numerous different models, with quite different parameter values, fit the observations equally well. Often we seek a certain combination of initial conditions and material properties that gives rise to some target geological behaviour. One approach to this task is inversion [Tarantola, 1987].

[3] Certain areas of geological modeling are amenable to numerical inversion, such as sedimentary basin evolution [e.g., Cross and Lessenger, 1999; Bellingham and White, 2000], in which available quantitative data (i.e., borehole logs and stratigraphic horizons from seismic interpretations) can be used for a direct measure of misfit. More often, however, the fit between geological observations and dynamic models is either too hard to describe mathematically, or open to considerable subjective interpretation, to the point where a single numer-

ical objective function cannot be specified. Thus we use an inversion procedure that depends on human interaction. The traditional numerical measure of data mismatch is replaced by the user's visual evaluation. This type of scheme is known as interactive evolutionary computation (IEC). A general overview of IEC appears in a review by *Takagi* [2001].

[4] We have applied this technique to several geological test cases [e.g., *Boschetti and Moresi*, 2001; *Wijns et al.*, 2003], with results exceeding our expectations based on past experience in optimizing nonlinear geophysical problems. We believe that the success lies, at least partly, in the subjective misfit evaluation. Rather than being a “toylike” replacement for an ideal numerical approach, the user's input provides the inversion process with more information than a simple numerical evaluation can provide. An expert eye can evaluate the global appearance of a solution, as well as details, and may deem a result “good” despite the presence of other negative features. The convergence seems to benefit greatly from this information.

[5] While the end product of most inversion procedures is a single best solution, many solutions are generated during the course of the process. The focus of this paper is on maximizing the information to be gained from an analysis of all solutions. Since the user ranks each solution, rather than lose this information at the end of the inversion run, we use it to obtain some understanding of the parameter space, which leads to a better understanding of the dynamical problem. From several statistical tools that are available to perform such an analysis, we choose a visual approach. The reason is twofold: first, geoscientists are trained and comfortable in using maps, and second, this provides a further level of interactivity between the user and the inversion process. The user not only judges the quality of each individual solution, but follows the inversion progress, and eventually, may control the direction of parameter exploration. Further benefits are explained in the Discussion section.

[6] We have adopted a technique known as self-organized mapping [*Kohonen*, 2001] as a means to

illustrate, via the use of a few simple plots, the roles of individual parameters in contributing both to “bad” solutions, and to the nonuniqueness of “good” solutions. We illustrate this approach using a geodynamic investigation of fault spacing during extension of the Earth's crust.

2. Self-Organized Map

[7] A self-organized map (SOM) is a transformation of high-dimensional (nD) data into a lower-dimensional (usually 2-D) plot. Broadly speaking, its aim is to spread nD points over a plane in such a way that topology is respected, i.e., two points lying close to one another in the higher-dimensional space should lie close in the 2-D plot. In doing so, it acts as a classification algorithm that separates all the input data into clusters according to similarity.

[8] The description and analysis of the mathematics underlying a SOM can be found both in the neural network literature and in the framework of statistical clustering tools. Because of its simplicity, we prefer to just describe the algorithm, which will help to highlight both the power and limitations of the technique. Given that we want to visualize a set of m data points in nD , the algorithm is summarized in the following steps:

[9] 1. Generate a (2-D) grid. This grid can have different shapes and sizes, and its nodes can also have different shapes. Our example uses a grid with hexagonal nodes, which allow contact with more nearest neighbors than rectangular nodes. The optimal number of nodes to represent m data points is determined via a heuristic calculation, in the absence of any established theory.

[10] 2. Initialize each node by assigning it a random nD vector of the same dimensionality as the data points. We will call these SOM vectors.

[11] 3. Pick one data point and find the SOM vector that is closest to the data point according to a certain metric (usually a simple Euclidean distance after normalization of the data set). We call this node the best matching unit (BMU). Modify the SOM vector belonging to the BMU by a certain amount so that it is closer (more similar) to the data point.

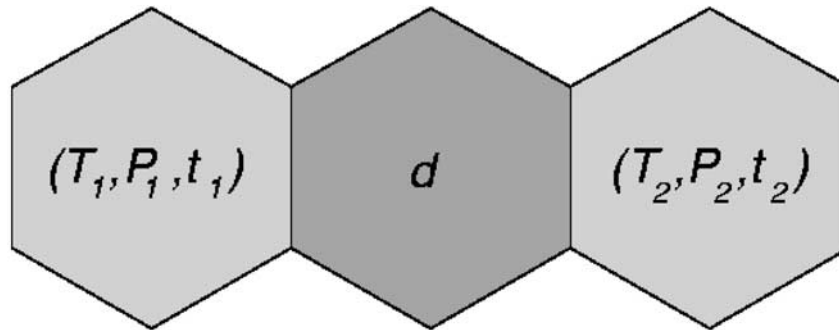


Figure 1. Illustration of nodes in a SOM. Two 3-D SOM vectors (T_1, P_1, t_1) and (T_2, P_2, t_2) , separated by a distance d , belong to two SOM data nodes. The distance node that connects the data nodes is colored according to the magnitude of d . Data nodes are also colored, using an average of surrounding distance nodes, for a more continuous display.

[12] 4. Choose a neighborhood of the BMU over the grid. The SOM vectors belonging to this neighborhood are also modified to be closer to the data point, by an amount inversely proportional to their grid distance to the BMU, i.e., the farther the location of the vector on the SOM grid, the less it is incremented.

[13] 5. Repeat items 3 and 4 for each point in the data set.

[14] 6. Iterate items 3 to 5 several times (usually a few thousand) to ensure convergence.

[15] The result of this algorithm is that SOM vectors belonging to nearby grid locations will tend to be similar, since they will tend to converge toward similar data points. Conversely, data points that are close to one another will tend to fall in grid nodes close to one another, or in the same grid node. This should achieve the dual purpose of clustering similar points and giving a best approximation of the original topology in the n D space. In practice, all parameter values are normalized according to their data extents before any calculations are made. Thus each component is equally weighted in the determination of distance.

[16] Clearly, what a SOM tries to achieve (mapping n D points into 2-D) is impossible except for trivial cases. Consequently, the final result is often non-optimal. The SOM depends on a number of parameters that control the algorithm described above. These include the number of grid points, the initialization of the SOM vectors, the amount by

which SOM vectors are updated toward the data point, the size of the BMU neighborhood, and the metric used to calculate distances. No standard values for these parameters exist in the literature, and their choice is problem specific and often left to the user's discretion. Also, because the SOM grid is not tied to any specific reference location in the n D space, e.g., the center of the SOM is not the center of the n D space, the appearance of maps with different initializations may be very different. The Web site <http://davis.wpi.edu/~matt/courses/soms/applet.html> offers an illustration of the effect of different parameter choices. Provided satisfactory convergence has been achieved, the relationship between adjacent clusters should still be represented in a relatively homogeneous way, and a trained user will recognize this.

[17] The SOM display that we use employs two different types of nodes: *data nodes* and *distance nodes*, illustrated in Figure 1. The data nodes represent the SOM vectors at the grid locations described above. The distance nodes connect the data nodes, and indicate the relative n D distance between adjacent SOM vectors. The distance nodes are colored to show the magnitude of the distance between adjacent nodes. Data nodes are also colored, according to an average of surrounding distance nodes, to produce a more continuous map. Colors representing short distances indicate clusters of close points, while colors representing large distances show cluster borders, which can also be interpreted as steep ridges dividing valleys of similar points.

[18] SOMs have been extensively employed in recent years in both scientific and engineering applications in order to visualize high-dimensional data and highlight data structure and clustering. We use a SOM for displaying the results of a 6-D inversion problem, where the input data are the rheological parameter sets used to generate numerical models of extensional faulting in the Earth's crust. The SOM plots have been produced with the use of the Matlab[®] SOM Toolbox, written by Juha Vesanto. More details about SOMs, and the specific implementation used in this work, can be obtained at the SOM Toolbox Web site <http://www.cis.hut.fi/projects/somtoolbox>.

3. Inverse Modeling of an Extensional Faulting Problem

[19] We explain the inversion and visualization process using an example of faulting during crustal extension. The goal is to find one or more sets of material parameters that give rise to fault spacing wider than the thickness of the upper crust, as sketched in Figure 2a. We are looking for well-defined faults that accommodate highly localized shear, using forward modeling software (a particle-in-cell finite element code) that is suited to problems involving large deformation [Moresi *et al.*, 2001, 2002]. An explanation of the code is on the Web site <http://www.ned.dem.csiro.au/research/solidMech/PIC>, along with example applications. Rheological controls on fault spacing are the subject of many analogue and numerical modeling studies [e.g., Benes and Davy, 1996; Thibaud *et al.*, 1999; Spadini and Podladchikov, 1996; Bai and Pollard, 2000]. The results we generate are fairly simple and are intended to illustrate the method. Wijns *et al.* [2003] provide a complete description of the numerical model and inversion process for a very similar extensional faulting problem. We confine ourselves here to a short summary.

[20] Figure 2b contains the initial model geometry. The visco-plastic upper crust, with strain-weakening behaviour, is 15 km thick. This overlies the top 6 km of a weaker, ductile lower crust. Above these is a highly compressible layer of low density, low

viscosity background material (“air”), which does not interfere with the mechanics of the problem. Extension proceeds by applying a uniform velocity to the right-hand boundary, equivalent to an average strain rate of 10^{-15} s^{-1} .

[21] The six model parameters that are allowed to vary are the viscosity η of the upper crust, and five yield parameters that describe the brittle (plastic) failure of the upper crust. These are the cohesion B_o , the pressure dependence B_p of the maximum sustainable shear stress, which is equivalent to the friction coefficient in Byerlee's Law [Byerlee, 1968], the tensile limit B_c of the crustal rocks, the maximum proportion of strain weakening E_a , and the “saturation strain” E_o beyond which no further weakening takes place.

[22] Six generations of models are run, with eight simulations per generation. At each generation, the user ranks the output images against the conceptual target in Figure 2a, looking for general behaviour and relative fault spacing rather than trying to reproduce the image exactly. In fact, the location and geometry of faults is extremely sensitive to initial perturbations, both in nature and in our numerical models, so that instead of devising a single numerical target, we depend on “multi-criteria” human evaluation. The rankings are then fed into a genetic algorithm, which chooses parameters for the next generation of simulations. The procedure stops when one or more satisfactory matches have been found. The bottom panels of Figure 2 show the progression of the outputs and the rankings accorded to each image, for the first, second, and sixth (last) generation of the inversion process. By the sixth generation, several images appear very similar, and represent “satisfactory” solutions.

4. SOM Visualization of the Inversion Data

[23] The input data for the SOM visualization consist of 48 points in a 6-D space, or 48 vectors of six components each. The components are the variable parameters described in the section above, namely, η , B_o , B_p , B_c , E_a , and E_o . These data are the output of six generations of eight simulations

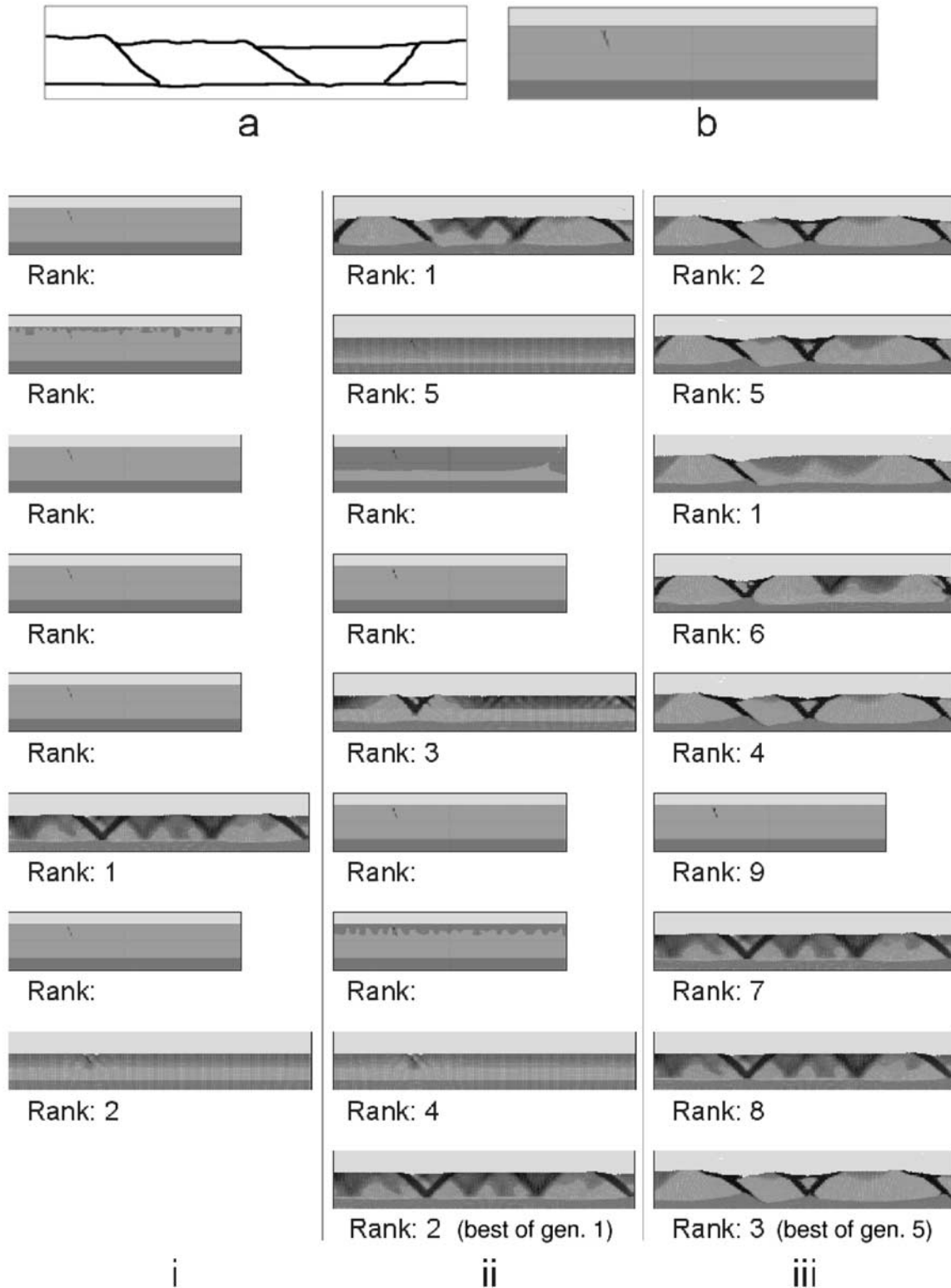


Figure 2. (a) Conceptual target, (b) initial geometry of the crust, and (c) evolution of the inversion. Panels (i) to (iii) represent the first two and the last (sixth) set of solutions generated by the algorithm. Images are ranked according to their fault spacing, where dark areas in the upper crust indicate accumulated plastic strain (faults). Models that have not been extended to full length because of numerical nonconvergence are left unranked. The third image of generation six (panel iii) is considered the best result, with the greatest fault spacing.

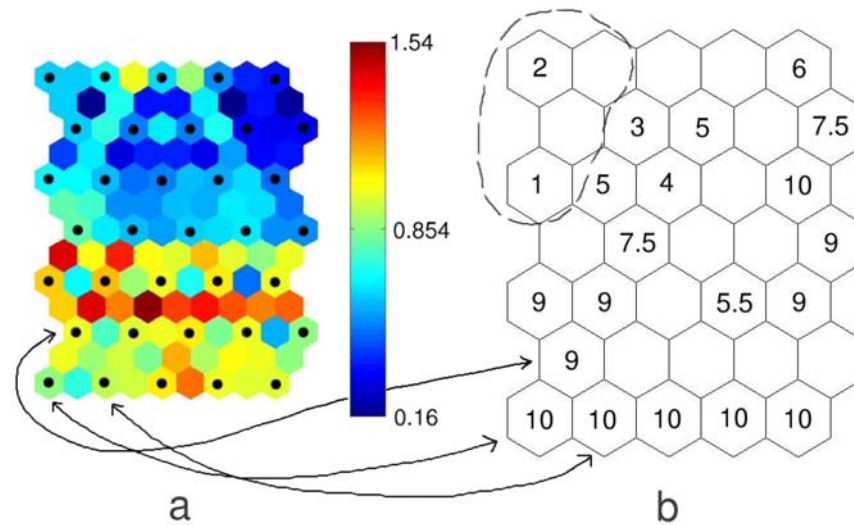


Figure 3. SOM of the extensional faulting data. (a) Every second node, indicated by a superimposed dot, is a data node. The data nodes are separated by distance nodes that indicate the difference between neighboring SOM vectors. The color bar shows the distance scale. The data nodes are also colored, according to an average of surrounding distance nodes. (b) Only data nodes are present, and labeled with an absolute ranking in terms of similarity between simulation results and the visual target. Unlabeled nodes are not associated with any input vectors. The dashed line encircles the domain of best model results. Arrows illustrate three equivalent data nodes between the two displays.

each, and represent the way in which the inversion procedure has sampled the parameter space.

[24] Figure 3a contains the main SOM plot, which is made up of both data nodes and distance nodes. Thirty-five data nodes, indicated by superimposed dots, are considered optimal to classify the 48 input vectors. Depending on the convergence, each SOM node may correspond to one or more of the 48 output images from the simulations, or it may be “empty”, meaning that no data point is close to it. The data nodes are separated by distance nodes, which are colored according to the distance between vectors as explained in the introduction to the SOM. A small distance connects locations whose SOM vectors are very similar. The data nodes are also colored, according to an average of surrounding distance nodes, for continuity of the display. A cluster in the SOM may be recognized as any collection of darker blue nodes that is bounded by light blue to red nodes. Such an area represents a domain of similarly parameterized extension models. Equivalent grayscale images, suitable for printing in black and white, are available from <http://www.ned.dem.csiro.au/Boschetti-Fabio/3054CO/papers/SOM-greyscale.pdf>.

[25] The original data vectors can be represented on the SOM by plotting each point at the grid location of its corresponding BMU (the grid node that is most similar to it). In order to identify the different model outputs, we have labeled all extension images with an overall rank at the end of the entire inversion exercise (Figure 3b). Well ranked solutions (closer to 1) are similar to the target. Unlabeled nodes are empty, as described above. It is clear that the top left domain, encircled with a dashed line, contains the best cluster of model images.

[26] Figure 4 illustrates the mapping of the output images onto the SOM. Both data nodes and distance nodes are included, as in Figure 3a, and the output images are labeled with their absolute rank. It is again clear that the area in parameter space at the top left corner contains the solutions most closely resembling the target image. At this point one may observe, for example, that while model 5.5 in Figure 4 is far from the “best” corner, being separated by a ridge, it nevertheless shares characteristics of the best models. This may be indicative of either the nonuniqueness of inversion solutions (models with very different parameter inputs may

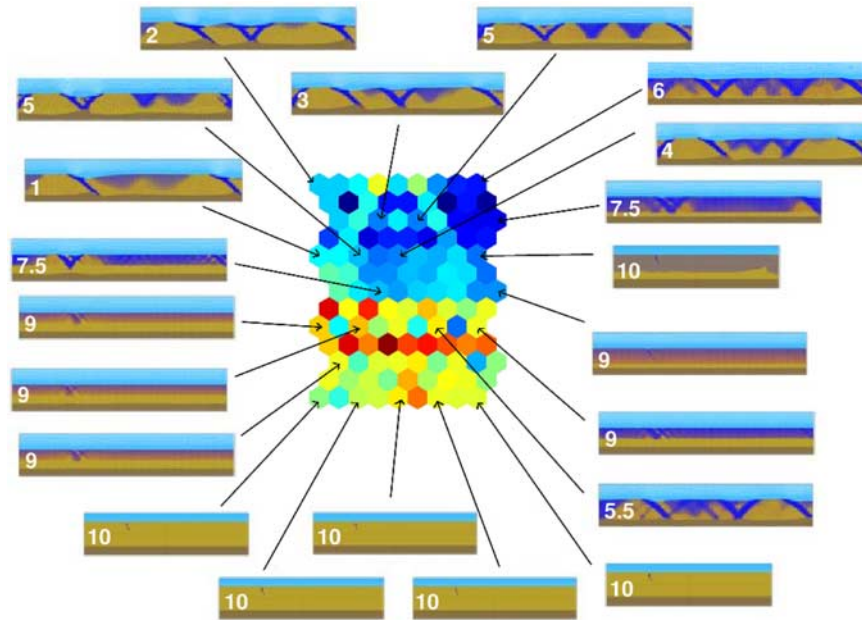


Figure 4. Mapping of model outputs onto the SOM grid of Figure 3a. Data nodes (every second node) represent outputs from the inversion process, as illustrated by the mapped images. The images are labeled with their absolute rankings (see Figure 3b). The best solutions are clustered in the top left domain.

produce similar outputs) or of a nonoptimal SOM clustering. In either case, the SOM suggests that this may be an area of parameter space that merits further investigation.

[27] In order to analyze the influence of each model parameter on the solution, we map the individual dimensions onto the SOM network of data nodes. The images in Figure 5 show the (nondimensional) nodal magnitude of each model parameter in the 6-D space. Viscosity shows increasing values from the bottom right corner toward the top left. Similar regular patterns can be seen for other parameters. When compared to the labeled SOM of Figure 3b, these parameter plots show the component values associated with each solution obtained during the inversion. There is a clear correlation between the best model images and a high viscosity. Although the best domain has consistently low values for the other five parameters, these have a less strict control, since low values also allow for models farther from the target image. The plots in combination could be summarized as follows, converting to natural parameter values: the best matches to the target image are achieved with a high viscosity $\eta > 5 \times 10^{22}$ Pa-s, and a low cohesion $B_o < 5$ MPa. The low friction

coefficient B_p (0.2–0.3), significant strain weakening E_a (0.2–0.3), and fairly rapid rate of weakening E_o (0.3–0.4) imply overall weak faults, as has been suggested for major structures [Bird and Kong, 1994; Bird, 1995; Lachenbruch and Sass, 1980, 1992]. Physically, this would promote large fault spacing by ensuring that once a fault is initiated, extensional stresses to either side quickly drop to below yield values, so that new faults do not form nearby. The tensile limit (2–6 MPa) may vary somewhat in the lower part of its range, again indicating weak rocks, although this should only have an effect near the surface, where the pressure may reach zero. Such a summary emerges quite naturally from the SOM analysis.

[28] In Figure 6 we show a combined representation of the individual parameter plots of Figure 5. The height of each bar indicates the normalized magnitude of each component of the SOM vector at every node. The order of the bars at each node refers again to the same order of the dimensions as in Figure 5. It is easy to understand the distance between SOM data nodes by comparing bar charts. Figure 6 confirms that a large viscosity is essential for producing the best model (shown by the arrow), together with relatively small values for the other

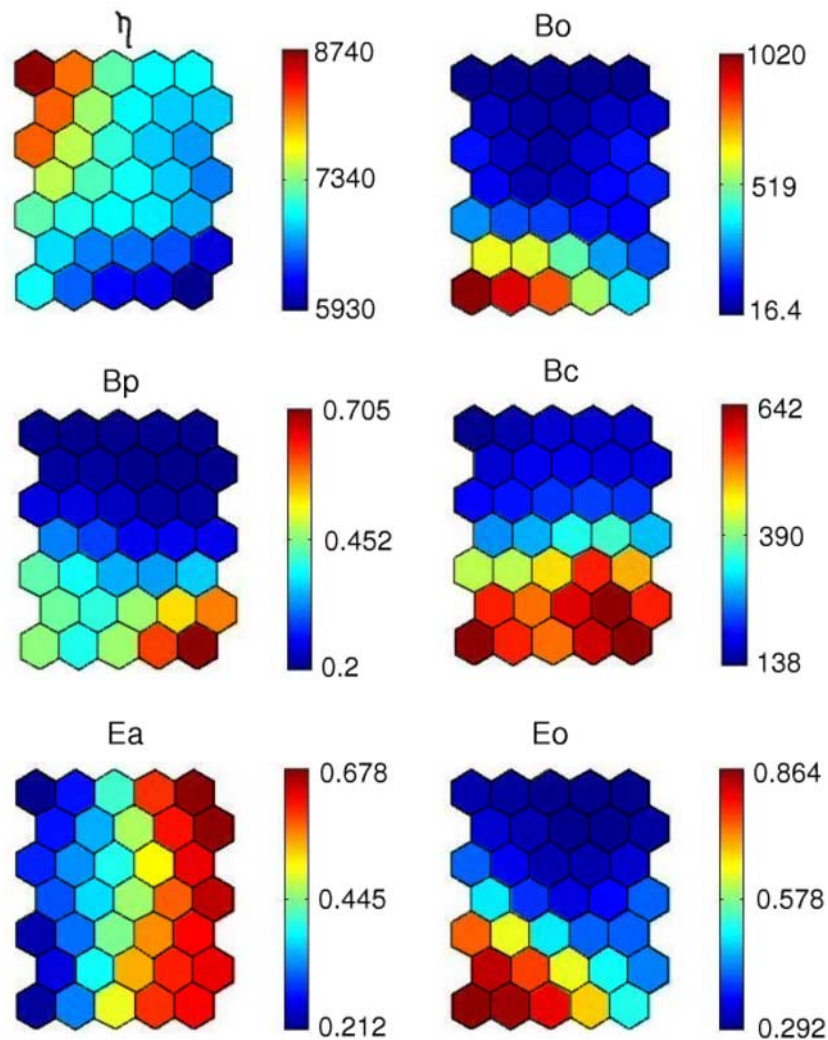


Figure 5. Individual parameter plots, data nodes only. The magnitude of each separate variable is shown at each data node in the SOM. Variables are the viscosity η , cohesion B_o , friction coefficient B_p , tensile strength B_c , maximum proportion of strain weakening E_a , and saturation strain E_o beyond which no further weakening takes place.

five components. Notice that the worst solutions (bottom) are not dictated by any one component, e.g., a high cohesion B_o , by itself, does not imply a bad solution. An unphysically high yield stress, through a combination of high cohesion and pressure dependence, is responsible for the models that failed to converge numerically (labeled “10” in Figure 4). Either of Figures 5 or 6 allows a quick scan of the parameter controls on model outputs.

5. Discussion

[29] Geoscientific problems, and geodynamic ones in particular, are among the most difficult inverse

problems. Their full solution is beyond not only today’s computational power, but also today’s mathematical tools. The combination of interactive inversion and visualization that we propose is not a panacea. Rather, it should be seen as a step in the delivery of a satisfactory approach. In this respect, the technique offers a number of advantages, some quite obvious, some less so.

[30] The SOM is a successful method of displaying high-dimensional data, and provides a way to deal with the many solutions that are generated by an inversion process. It produces relatively simple plots which are useful for determining which

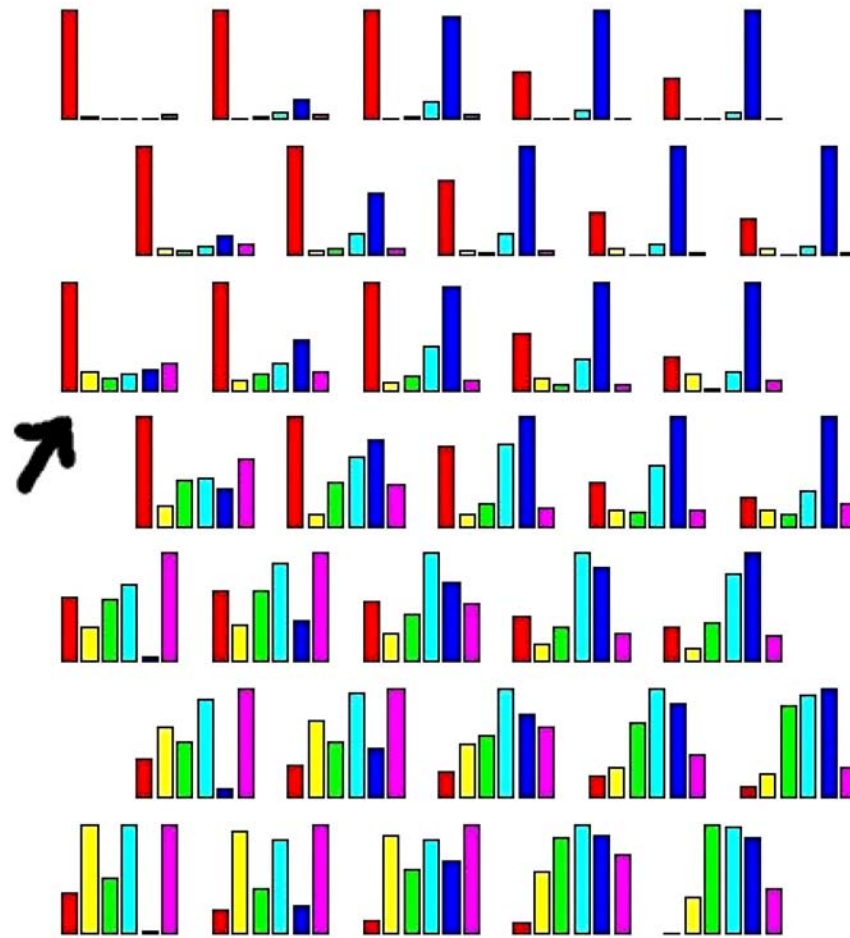


Figure 6. Visualization of the normalized SOM vectors at each data node. The order of the bars refers to the same order of the parameters as in Figure 5, namely η , B_o , B_p , B_c , E_a , and E_o . The arrow indicates the best model output.

parameters most affect the process under study. Related to this is the determination of which mechanical behaviors are possible given a certain modeling scenario. This is one focus of our current research.

[31] The approximate understanding of the search space can be used to further interact with the inversion itself. One obvious way is to remove parameters once they have been “optimized”, or parameters which are seen to have little impact on the models. This reduces the dimensionality of the problem. Another approach is to focus the search into smaller domains, where the “good” models lie. This can result in faster convergence as well as the opportunity to increase the search resolution of certain parameters. A user with a good knowledge of the inversion algorithm (a genetic algorithm in

this case) can also use the information of the current state of convergence in order to tune certain parameters controlling the inversion itself. The opportunity to do this “on line” can considerably improve performance. In the case of a genetic algorithm, this may involve changing the cross-over or mutation operator, or changing the number of individuals.

[32] The approach we describe can be a vehicle to facilitate the transfer of inversion technology to applied modelers. In our experience, the user-friendliness inherent in the approach (which removes the user from the underlying mathematics and allows him/her to concentrate on the geological aspects of the problem) has been very well received by industry representatives. It can be a crucial factor in the acceptance of geological mod-

eling as, for example, a mineral/oil exploration tool. There is also an educational benefit, allowing students to “see”, understand, and control the modeling and inversion process. We know of at least one geology department interested in this approach for an undergraduate course. Finally, this tool can be a vehicle for easier interaction and communication between “natural sciences oriented” and mathematically oriented geoscientists. It can help the first group to deal with esoteric concepts like *multidimensional manifolds*, *global* and *local minima*, and *ambiguity domains*, and the second group to appreciate the subtleties of the geological interpretation of results. The two users can interpret inversion solutions together, accounting for both their geological meaning and the quality of the inversion process.

6. Conclusion

[33] Geological modeling is inherently ill constrained and subject to a large number of unknown parameters, each with a possibly wide range of values. During inverse modeling, it is in the interest of the modeler to capitalize on the availability of accumulated solutions in order to understand the dynamics and nonuniqueness of the problem as fully as possible. Combined with the systematic ranking of trial solutions, we use a self-organized map (SOM) to represent our multidimensional parameter space in a clear and simple 2-D visualization environment. The SOM provides plots from which it is easy to draw conclusions regarding the controlling physical factors and the connections between them.

Acknowledgments

[34] The authors thank Dr. Roberto Weinberg for suggesting the short SOM tutorial to improve the clarity of the manuscript, and Dr. Andrew Curtis for helping to focus the paper on the visualization aspect.

References

Bai, T., and D. Pollard, Fracture spacing in layered rocks: A new explanation based on the stress transition, *J. Struct. Geol.*, 22, 43–57, doi:10.1016/S0191-8141(99)00137-6, 2000.

- Bellingham, P., and N. White, A general inverse method for modelling extensional sedimentary basins, *Basin Res.*, 12, 219–226, 2000.
- Benes, V., and P. Davy, Modes of continental lithospheric extension: Experimental verification of strain localization processes, *Tectonophysics*, 254, 169–187, 1996.
- Bird, P., Lithosphere dynamics and continental deformation, *U.S. Natl. Rep. Int. Union Geod. Geophys. 1991–1994, Rev. Geophys.*, 33, 379–383, 1995.
- Bird, P., and X. Kong, Computer simulations of California tectonics confirm very low strength of major faults, *Geol. Soc. Am. Bull.*, 106, 159–174, 1994.
- Boschetti, F., and L. Moresi, Interactive inversion in geosciences, *Geophysics*, 66, 1226–1234, 2001.
- Byerlee, J., Brittle-ductile transition in rocks, *J. Geophys. Res.*, 73, 4741–4750, 1968.
- Cross, T., and M. Lessenger, Construction and application of a stratigraphic inverse model, in *62 Numerical Experiments in Stratigraphy: Recent Advances in Stratigraphic and Sedimentologic Computer Simulations*, edited by J. Harbaugh et al., pp. 69–83, Soc. for Sediment. Geol., Tulsa, Okla., 1999.
- Kohonen, T., Self-organizing maps, in *Series in Information Sciences*, vol. 30, 3rd ed., Springer-Verlag, New York, 2001.
- Lachenbruch, A., and J. Sass, Heat flow and energetics of the San Andreas fault zone, *J. Geophys. Res.*, 85, 6185–6222, 1980.
- Lachenbruch, A., and J. Sass, Heat flow from Cajon Pass, fault strength, and tectonic implications, *J. Geophys. Res.*, 97, 4995–5015, 1992.
- Moresi, L., H.-B. Mühlhaus, and F. Dufour, Viscoelastic formulation for modelling of plate tectonics, in *Bifurcation and Localization in Soils and Rocks*, edited by H.-B. Mühlhaus, A. Dyskin, and E. Pasternak, pp. 337–344, A. A. Balkema, Brookfield, Vt., 2001.
- Moresi, L., F. Dufour, and H.-B. Mühlhaus, Mantle convection models with viscoelastic/brittle lithosphere: Numerical methodology and plate tectonic modeling, *Pure Appl. Geophys.*, 159, 2335–2356, 2002.
- Spadini, G., and Y. Podladchikov, Spacing of consecutive normal faulting in the lithosphere: A dynamic model for rift axis jumping (Tyrrhenian Sea), *Earth Planet. Sci. Lett.*, 144, 21–34, 1996.
- Takagi, H., Interactive evolutionary computation: Fusion of the capacities of EC optimization and human evaluation, *Proc. IEEE*, 89, 1275–1296, 2001.
- Tarantola, A., *Inverse Problem Theory*, 613 pp., Elsevier Sci., New York, 1987.
- Thibaud, R., O. Dauteuil, and P. Gente, Faulting pattern along slow-spreading ridge segments: A consequence of along-axis variation in lithospheric rheology, *Tectonophysics*, 312, 157–174, 1999.
- Wijns, C., F. Boschetti, and L. Moresi, Inverse modelling in geology by interactive evolutionary computation, *J. Struct. Geol.*, 25(10), 1615–1621, doi:10.1016/S0191-8141(03)00010-5, 2003.